Fracture Mechanics of Concrete Structures,
Proceedings FRAMCOS-2, edited by Folker H. Wittmann,
AEDIFICATIO Publishers, D-79104 Freiburg (1995)

FURTHER STUDIES OF THE FRACTURE PROCESS ZONE ASSOCIATED WITH MIXED MODE DYNAMIC FRACTURE OF CONCRETE

Z. K. Guo, M. Kosai, A. S. Kobayashi
Department of Mechanical Engineering,University of Washington, Seattle, Washington, USA
N. M. Hawkins
Department of Civil Engineering, University of Illinois at Urbana-Champaign, Urbana, Illinois, USA

Abstract

The fracture process zone associated with rapid crack propagation in an impacted, three-point bend (TPB), concrete specimen with an off-set precrack was analyzed by a hybrid dynamic Moire interferometry/dynamic finite element analysis. The crack kinked and propagated with increasing dynamic mode I resistance, K_I^{dyn}, but with negligible K_{II}^{dyn}. The crack sliding resistance was undetectable in the FPZ but the crack opening resistance increased under this mixed modes I and II loading.

1 Introduction

The fracture process zone (FPZ), as defined in an ACI report (1992), is the "zone in which the material undergoes strain-softening" and is related to the strip yield or cohesive force zone in ductile fracture of metals. Hillerborg et al (1976, 1985) designated this cohesive force zone approach in concrete as the fictitious crack model where the traction-free crack opens upon reaching the tensile strength, f_t', and propagates when the fracture energy, G_f, exceeds a critical value. The softening curve, which

relates the crack closing stress (CCS) versus crack opening displacement (COD) in the FPZ, has been modeled theoretically by Horii et al (1989) and Bazant (1987) and experimentally by Du et al (1990). Theoretically the fictitious crack model requires only a single parameter of f_t for stable crack growth of the crack tip of a traction free crack. In practice, however, this crack tip cannot advance without the extension of the FPZ crack tip and thus requires an additional critical G_f for crack propagation.

The two-parameter fracture criterion of Jenq et al (1985, 1987), which models the FPZ effect by a critical crack tip opening displacement, d_t, is appealing since it retains the linear elastic fracture mechanics aspect of concrete fracture through a critical stress intensity, factor, K_{IC}. This criterion has been extended to mixed Modes I and II fracture of concrete by replacing the Mode I stress intensity factor, K_I, with an effective stress intensity factor, $K_I^2 = [K_I^2 + K_{II}^2]^{1/2}$ and the vector sum of the opening and sliding crack tip displacements .

The FPZ model with a crack tip singularity (Yon et al, 1990), referred to as the S-FPZ model, utilizes the FPZ of the fictitious crack model without the sharp rise in the CCS near the crack tip and a crack tip stress intensity factor similar to (Jenq et al, 1985). Experimental evidences (Guo et al, 1994a) indicate that the CCS versus COD relation characterizing the FPZ is not a material property and varies with the mechanical properties, loading condition and possibly the specimen geometry. Since stable crack growth and the onset of rapid fracture is governed by the critical stress intensity factor, K_{IC}, the S-FPZ model differs with Jenq et al (1985) in that it characterizes concrete fracture with a single parameter augmented by the CCS versus COD relation of that particular FPZ. The authors and their colleagues have used the S-FPZ model to analyze static and dynamic Mode I and mixed Modes I and II fracture of three-point bend and compact tension (CT) concrete specimens. The purpose of this paper is to present additional data to a recent paper (Guo et al, 1994b) and summarize our findings on dynamic mixed mode fracture of concrete.

2 Experimental procedure

2.1 Specimen

The single edge notched (SEN), three-point bend (TPB) concrete specimen, as shown in Fig. 1, differs with that of (Guo et al, 1994b) in that the machined crack is off-set 57.2 mm from the line of symmetry or the load line. The concrete specimens, however, were casted together with those of (Guo et al, 1994b) and consists of a high early-strength Portland cement (Type III), local sand, aggregate and water mixed in the proportion of

1:3:2:0.5, respectively. The average gradation of the sand was based on ASTM C-404 Size No. 1 and the

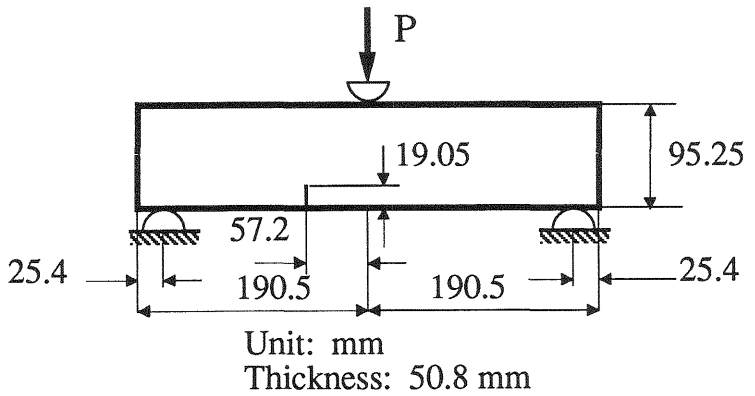

Fig. 1. SEN three point bend concrete specimen

maximum gravel size was 6.4 mm. A moire with vertical and horizontal diffraction grating of 600 lines per mm was transferred to the polished specimen surface and five strain gages were installed on the other unpolished surface along the predicted crack path. The specimens were then precracked under mode I loading such that the influence of a pre-existing, Mode I fracture process zone (FPZ) on the mixed modes I and II fracture could be studied.

2.2 Test procedure

A drop weight tester with a 10-kilogram impactor and a drop height of 1 meter was used to generate a moderately high-strain rate loading. The concrete specimen was also instrumented with a dynamic load cell at the impact point and two non contact displacement gages at the load point on both sides of the specimen. The two displacement gages provided an average load-line displacement data and accounted for the uneven crush of the specimen at the impact point.

Eight pairs of the orthogonal displacement fields associated with the moire patterns of a propagating crack were recorded simultaneously by two ultra-high speed IMACON 790 cameras with an exposure time of 2 ms. and at a framing rate of 100,000 frames/sec. In addition, the impact load, load-line displacement and five strain gage readings along the anticipated crack path were recorded. The crack kinked immediately upon propagation and the total fracture event, which lasted about 1.5 ms., was reconstructed by assembling a composite record of four identical fracture tests with varying time delay in triggering the two cameras.

2.3 Numerical analysis

An elastodynamic finite element (FE) code was used in its propagation to determine the crack closing stress (CCS) versus crack opening displacement (COD) as well as the crack shearing stress (CSS) versus crack sliding displacement (CSD) relations in the FPZ trailing the rapidly propagating crack. The procedure consisted of iterating assumed CCS versus COD and CCS versus CSD relations until the computed COD and CSD coincided with their measured counterparts. Energy dissipated in the FPZ was obtained through the work done by the CCS acting on the COD and the CSS acting on the CSD. The energy dissipation rate together with the energy release rate, kinetic energy rate and the external work rate were computed directly in the FE analysis.

3 Results

The load variations with time of the four specimens, which are designated as MB4-4, MB4-6, MB4-14 and MB4-16, are shown in Fig. 2 and the corresponding crack paths are shown in Fig. 3. The excellent agreements in the loads and crack paths of the four specimens indicate that the tests were reproducible and justifies the use of an average load and crack path histories, shown in solid curves in Figs. 2 and 3, respectively, for numerical analysis. The static tensile strength and static modulus of elasticity, which were obtained from compression cylinder tests, were 3.14 MPa and 31.9 GPa, respectively. The static and dynamic Poisson ratio was assumed to be 0.15.

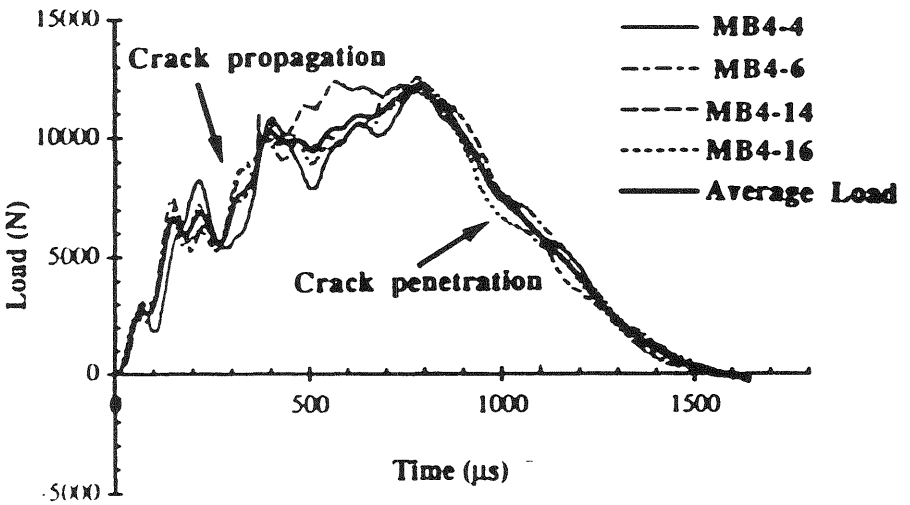

Fig. 2. Load history of four tests

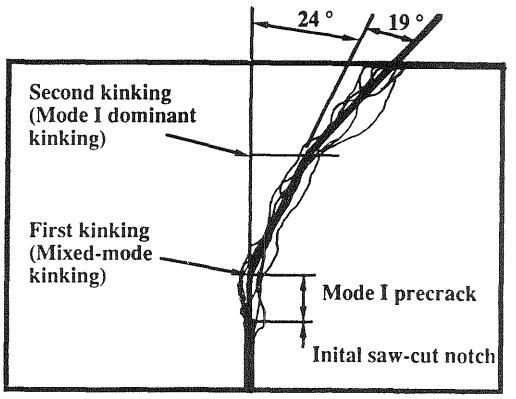

Fig. 3. Crack paths

The five average strain gage data along the crack paths of the four specimens are shown in Fig. 4 together with the corresponding computed strains. The diverging strains signal the passage of the crack tip. The crack tip location, which was deduced from the strain gage data and the moire fringe records, as a function of time was then used to drive the FE model of the fracturing concrete specimen. The maximum crack velocity obtained from this crack tip history was 250 m/s which is about 12% of the distortional wave velocity of concrete. A static crack tip analysis of this dynamic event, at most, will result in about 2% in an overestimated stress intensity factor.

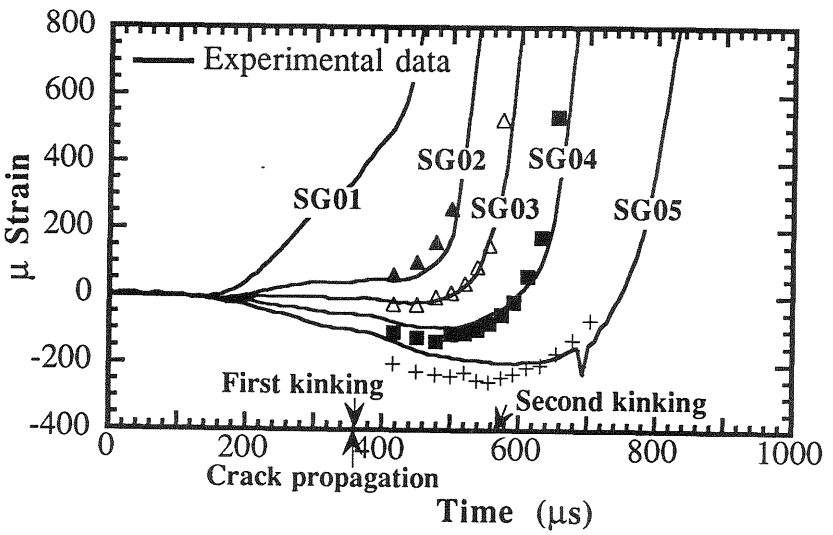

Fig. 4. Measured and computed average strain history

Figure 5 shows a composite measured and computed u_X and u_Y record of the propagating kinked crack. Only qualitative matches between the measured and computed crack profiles can be expected since the recorded instantaneous crack length does not necessary coincide with the incrementally extended FE crack length. The actual COD and CSD of the kinked crack were computed by local coordinate transformation of u_X and u_Y are shown in Fig. 6.

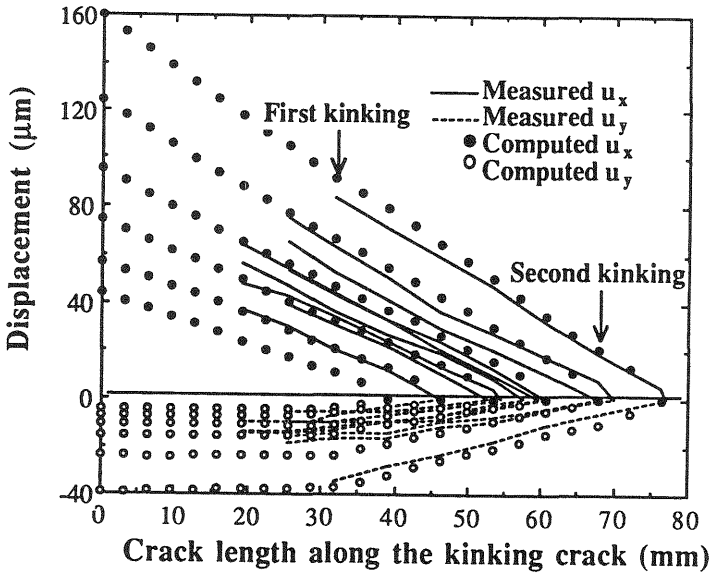

Fig. 5. Measured and computed u_X and u_Y

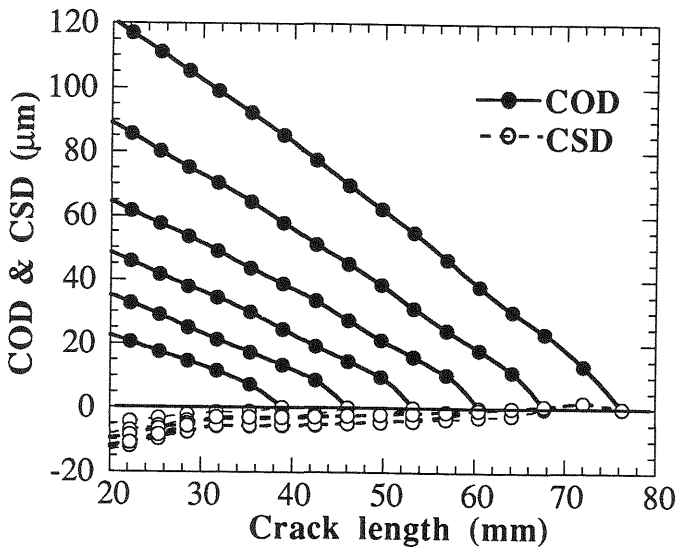

Fig. 6. COD and CSD variations

Figure 7 shows the CCS versus COD relation which yielded the correct u_x and u_y displacements in Fig.6. Also shown in Fig. 7 for comparison are the CCS versus COD relations of a previous dynamic and static mixed mode studies. These static and dynamic results of different crack offsets show that the resistance to crack sliding under mixed modes I and II crack tip deformation is negligible in comparison to the CCS. However, the presence of the small sliding resistance was noted through the increase in CCS over the CCS in identical specimens subjected to pure mode I loading (Guo et al, 1994a) The other adjustable parameter in this inverse dynamic FE analysis was the dynamic modulus of elasticity of which 47.5 GPa provided the correct u_x and u_y.

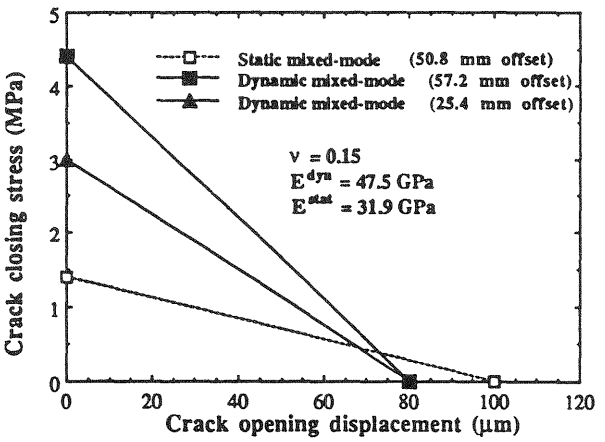

Fig. 7. CCS versus COD relations for mixed mode concrete fracture

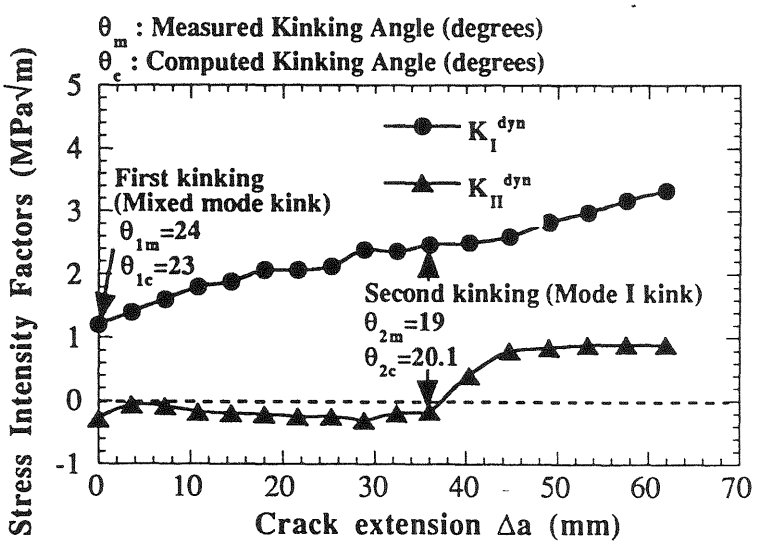

Fig. 8. K_I^{dyn} and K_{II}^{dyn} variations with crack extension

Figure 8 shows the variations in dynamic stress intensity factors, K_I^{dyn} and K_{II}^{dyn} or the resistance curves. The kinked crack propagated under mode I condition with increasing K_I^{dyn} but with negligible K_{II}^{dyn}. However, unlike our static mixed-mode crack growth study (Guo et al, 1994a) K_{II}^{dyn} in this as well as our previous dynamic mixed mode study [11] with an 25.4 mm offset crack rose to a significant value after the second kinking.

Figure 9 show the changes in energy partition with rapid and kinked crack propagation. The difference between the external work and the total energy in the specimen is almost identical to the energy dissipated in the FPZ. Thus the FPZ is the dominant energy dissipation mechanism in concrete fracture. In previous papers, we attributed the observed differences between the dissipated energy at the FPS and the total energy in the fracture specimen to the energy dissipated by aggregate/mortar interface cracking ahead of the propagating crack tip and local crushing at the load and support points. This energy balance conjecture was in error since we did not account for the energy stored in the FPZ.

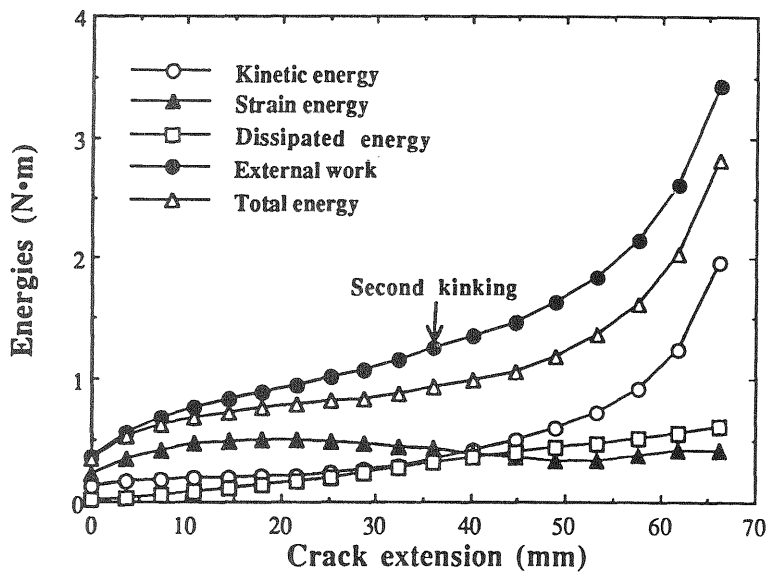

Fig. 9. Energy partition with crack extension

4 Crack kinking

Following the validation procedure used in (Guo et al, 1994a, 1994b), the crack kinking angles were estimated from the dynamic crack tip stress field obtained from dynamic FE analysis using the Ramulu's crack kinking

criterion (Ramulu et al, 1983) extended for crack growth under mixed mode fracture (Shimamoto et al, 1994). The two predicted and measured crack kinking angles are listed in Fig. 8 The excellent agreement between the measured and FE computed angles provide further credibility to the hybrid experimental-numerical procedure used in this study.

5 Conclusions

1. The CCS versus COD relation governing the FPZ of a propagating crack in a concrete specimen stiffened under dynamic fracture and with the severity of mixed mode loading.
2. The CSS was negligible but contributed to the stiffening of the CCS versus COD relation.
3. The FPZ is the dominant source of energy dissipation mechanism in concrete fracture.

6 Acknowledgement

This reserach was supported by the Air Force Office of Scientific Research Grant AFOSR-01-0218 and F49620-93-1-0210. The authors wish to thank Drs. Spencer Wu and Walter F. Jones for their valuable advice during the course of this investigation.

7 References

ACI Committee Report 446, Fracture Mechanics (1992) Fracture mechanics of concrete: concepts, models and determination of material properties in **Fracture Mechanics of Concrete Structures** (ed Z. P. Bazant), Elsevier Applied Science, 3-140.

Bazant, Z.P. (1987) Snapback instability at crack ligament tearing and its implication for fracture mechanics. **Cement and Concrete Research,** 17, No. 6, 951-967.

Du, J.J., Kobayashi, A.S. and Hawkins, N.M. (1990) An experimental-numerical analysis of fracture process zone in concrete fracture specimens. **Engineering Fracture Mechanics,** 35, No. 1/2/3, 15-27.

Guo, Z.-K., Kobayashi, A.S. and Hawkins, N.M. (1994a) Mixed modes I and II concrete fracture - an experimental analysis. **ASME J. of Applied Mechanics,** 61, 815-821.

Guo, Z.K., Kobayashi, A.S. and Hawkins, N.M. (1994b) Fracture process zone in mixed mode dynamic fracture of concrete in **Fracture and Damage in Quasi-Brittle Structures** (eds Z. Bazant, Z. Bittnar, M. Jirasek and J. Mazars), E.F. Spon, London, 217-230.

Hillerborg. A. (1985) The theoretical basis of method to determine the fracture energy *Gf* of concrete. **Materials and Structures,** 18, No. 106, 291-296.

Hillerborg, A., Modeer, M. and Petersson, P.E. (1976) Analysis of crack formation and crack growth in concrete by means of fracture mechanics and finite elements. **Cement and Concrete Research,** 6, 773-782.

Horii, H., Hasegawa, A. and Nishino, F. (1989) Fracture process and bridging zone model and influencing factors in fracture of concrete in **Fracture of Concrete and Rock** (eds S.P. Shah and S.E. Swartz), Springer-Verlag, 205-219.

Jenq, Y.S. and Shah, S.P. (1985) Two-parameter fracture model for concrete. **J. of Engng Mechanics, ASCE,** 111, No. 12, 1227-1241.

Jenq, Y.S. and Shah, S.P. (1987) Mixed mode fracture parameters of concrete in **Proc. of SEM-RILEM Int. Conf. on Fracture of Concrete and Rock** (eds S.P. Shah and S. Swartz), Soc. of Experimental Mechanics, 359-369.

Ramulu, M. and Kobayashi, A.S. (1983) Dynamic crack curving - a photoelastic evaluation. **Experimental Mechanics,** 20, 17-23.

Shimamoto, A., Kosai, M. and Kobayashi, A.S. (1994) Crack arrest at tear straps under mixed mode loading. **Engineering Fracture Mechanics,** 47, 59-74.

Yon, J.-H., Hawkins, N.M. and Kobayashi, A.S. (1990) Singular-FPZ model for numerical simulation of dynamic fracture of concrete in **ECF 8 Fracture Behavior and Design of Materials and Structures, Vol. II** (ed. D. Firrac), 618-625.